Lyle, M., Koizumi, I., Richter, C., and Moore, T.C., Jr. (Eds.), 2000
Proceedings of the Ocean Drilling Program, Scientific Results, Vol. 167

31. *DATA REPORT:* CORRECTION OF INDEX PROPERTIES AND THE METERS COMPOSITE DEPTH SCALE USING ELASTIC PROPERTIES OF LEG 167 SEDIMENTS[1]

Kevin MacKillop[2]

INTRODUCTION

Drilling during Leg 167 at the California margin was scheduled to recover continuous sedimentary sections. Multiple advanced piston core (APC) holes drilled at different depth offsets provided core overlap in successive APCs. Correlation of high-resolution laboratory physical properties data from adjacent APC holes was used to compile composite depth sections for each site. The composite depth sections were used to confirm continuous recovery and enable high-resolution sampling. The meters composite depth (mcd) scale differs from the shipboard meters below seafloor (mbsf) scale because of (1) core expansion following recovery (MacKillop et al., 1995), (2) coring gaps, and (3) stretching/compression of sediment during coring (Lyle, Koizumi, Richter, et al., 1997). Moran (1997) calculated that sediment expansion accounted for 90%–95% of the Leg 154 depth offset between shipboard mbsf and the mcd scales.

Terzaghi's one-dimensional theory of consolidation (Terzaghi, 1943) describes the response of sediments to stress loading and release. Mechanical loading in marine environments is provided by the buoyant weight of the overlying sediments. The load increases with depth below seabed, resulting in sediment volume reduction as water is "squeezed" out of the voids in the sediment. Stress release during core recovery results in expansion of the sediment and volume increase as water returns to the sediment. The sediment expansion or rebound defines the elastic properties of the sediment.

In this study we examine the elastic deformation properties of sediments recovered from Sites 1020 and 1021. These results are used to (1) correct the laboratory index properties measurements to in situ values and (2) determine the contribution of sediment rebound to the depth offset between the mbsf and mcd scales.

METHODS

One-dimensional (vertical) consolidation tests were completed on seven samples recovered from Sites 1020 and 1021. Whole-round samples, 10 cm long, were cut from the core sections, capped, sealed in wax, and stored in refrigerated seawater until testing. The tests were conducted in two back-pressured consolidometers at the Bedford Institute of Oceanography. The application of back pressure redissolves air bubbles trapped within the sample. The samples were back pressured for a minimum of 12 hr before incremental loading was started. A standard load increment ratio of one was used, and the samples were double drained (top and bottom). The measured and derived index properties (Table 1), determined before the start of each test, were similar to those obtained at sea, indicating that no desiccation of the samples occurred during transport and storage. In addition, no disturbance was observed during sample preparation.

Table 1. Index physical properties data for consolidation samples.

Hole, core, section, interval (cm)	Depth (mbsf)	Water content (%)	Specific gravity	Initial void ratio
1020D-1H-4, 140-150	5.95	108.68	2.670	2.805
1020C-11H-2, 140-150	92.75	81.62	2.674	2.195
1020C-16H-5, 140-150	144.78	81.49	2.641	2.227
1021D-1H-3, 140-150	4.45	125.81	2.705	3.415
1021C-5H-2, 140-150	34.05	104.64	2.662	2.713
1021C-9H-1, 140-150	70.55	139.68	2.605	3.484
1021C-18H-3, 140-150	159.05	120.12	2.620	3.084

The consolidation test measures the change in sample height over a series of increasing (loading) and decreasing (unloading) stresses. The change in sample height is used to calculate the volume change expressed as void ratio. The consolidation results, plotted as a consolidation curve (Fig. 1), are used to determine the coefficient of expansion (C_r) defined as the log-linear slope of the rebound portion of the curve. The elastic rebound causes the bulk density and dry density to decrease while porosity and void ratio increases. The elastic rebound does not change the grain density or pore-fluid density. Discrete laboratory index data were corrected using the coefficient of expansion. Void ratio values were corrected to in situ values as follows:

$$e_c = e_i - [(\log P'_o) C_r], \quad (1)$$

where e_c is the corrected void ratio, e_i is the laboratory-determined void ratio, and P'_o is the effective overburden stress calculated using

$$P'_o = [d(\rho_c - \rho_w)9.81], \quad (2)$$

where d is the discrete measurement interval (mbsf), ρ_c is the laboratory-determined bulk density, and ρ_w is the pore-fluid density. Porosity values were corrected using the following phase relationship:

$$n_c = e_c/(1 + e_c). \quad (3)$$

Bulk density (ρ_c) and dry density (ρ_{dc}) data were corrected to in situ valves using corrected void ratio (e_c), grain density (ρ_g), pore-fluid density (ρ_w), and the following phase relationships:

$$\rho_c = [(\rho_g + e_c)/(1 + e_c)]\rho_w, \text{ and} \quad (4)$$

$$\rho_{dc} = \rho_g/(1 + e_c). \quad (5)$$

The corrected bulk density values can be used for constructing synthetic seismograms, determining in situ stress conditions, and correlating with downhole logging data. Corrected dry density data can be used in determination of mass accumulation rates.

The change in void ratio over one core length is geometrically related to the increase in core length or core expansion (MacKillop et al., 1995). The core length expansion (ΔL) in meters over discrete measurement intervals was calculated from the elastic change in void ratio as follows:

[1]Lyle, M., Koizumi, I., Richter, C., and Moore, T.C., Jr. (Eds.), 2000. *Proc. ODP, Sci. Results,* 167: College Station TX (Ocean Drilling Program).
[2]K&K Geoscience, 17 Hawthorne Street, Dartmouth, NS, B2Y 2Y4, Canada. Kevin.MacKillop@dal.ca

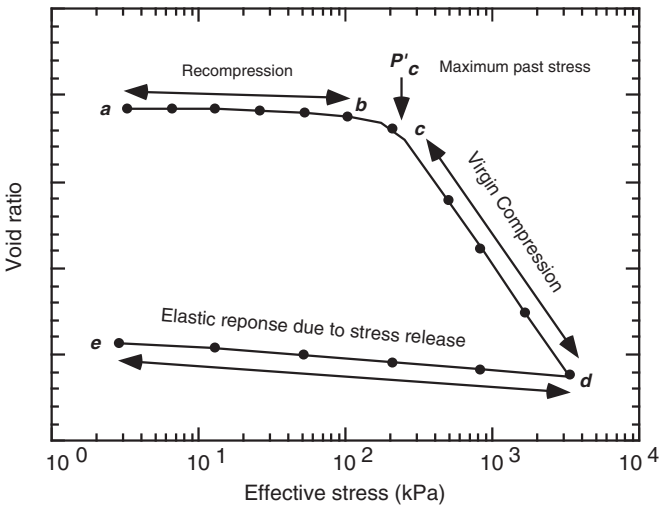

Figure 1. Example of a typical consolidation plot showing the recompression of the sample (a to b) to the preconsolidation stress (P'_c), the virgin compression curve (c to d), and the unloading curve (d to e).

$$\Delta L = \Delta e\ (L_o - nL_o), \tag{6}$$

where n is the core porosity and L_o is the recovered length of core. The ΔL over discrete measurement intervals is then accumulated and added to the mbsf scale. The accumulated length in meters below seafloor is then compared with the mcd scale.

RESULTS

Seven consolidation tests were completed on samples from Holes 1020C, 1021C, and 1021D. The test results (Table 2) show sharp transitions between the recompression and virgin compression curves (Figs. 2, 3). This suggests little sample disturbance (Holtz and Kovacs, 1981) and increases the accuracy of the preconsolidation (P'_c) stress determination. The elastic rebound values range from 0.067 to 0.087 for Site 1020 and from 0.067 to 0.085 for Site 1021. The consistent rebound values suggest little variation in the composition of the seven samples. Average elastic rebound values of 0.075 for Site 1020 and 0.077 for Site 1021 were used to correct void ratio to in situ values (Eq. 1). Tables 3 and 4 contain the corrected void ratio, bulk density, dry density, and porosity values for discrete measurements on APC cores for Sites 1020 and 1021.

The consolidation state of the sediment was determined from the overconsolidation ratio (OCR) values of each test. OCR is calculated by

$$\mathrm{OCR} = P'_c / P'_o. \tag{7}$$

The sediment is overconsolidated (OCR > 1) in the upper few meters and becomes normally consolidated (OCR ≅ 1) with depth. The only exception is at 92 mbsf (Section 167-1020C-11H-5), where the sediment is underconsolidated (OCR < 1).

The increase in core length over discrete measurement intervals was calculated from the elastic response change in void ratio (Eq. 6). This core-length expansion results in a recovery greater than the cored length and contributes to the depth offset between the mbsf and mcd scales. Following Moran (1997), the core-length expansion was used to correct the mcd scale to a more realistic depth. The cumulative core lengthening for Sites 1020 and 1021 (APC cores) was plotted as a function of meters below seafloor (Fig. 4). The elastic core expansion results are best approximated using a simple power function in the form of

$$E = a(\mathrm{mbsf}^b), \tag{8}$$

where E is the sediment rebound in meters and a and b are coefficients determined from the power function for each site (Table 5). The mcd scale was therefore corrected by removing the sediment rebound (i.e., mcd – E) from the mcd scale.

The corrected mcd scales for Sites 1020 and 1021 (Holes 1020B, 1020C, 1021B, and 1021C) are plotted against the mbsf scale (Figs. 5, 6). A one-to-one correlation between the mbsf and the corrected mcd (mcd_c) scales would indicate that sediment rebound accounts for 100% of the mcd offset. There is good linear correlation between the two scales. Moran (1997) calculated that elastic core expansion accounts for 90%–95% of the depth offset between the mbsf and mcd scales for Leg 154. Moran (1997) estimated that the remaining 5%–10% of the depth offset for Leg 154 results from intervals of sediment flow-in, identified in visual description of the split core. The percentage that sediment rebound contributes to the mbsf and mcd depth offset for Leg 167 varies from 40% to 80% (Tables 6, 7).

Table 2. Summary of consolidation test results.

Hole, core, section, interval (cm)	C_r	C_c	P'_o	P'_c	*OCR*
1020D-1H-4, 140-150	0.067	0.76	31.65	155	4.90
1020C-11H-2, 140-150	0.087	0.80	479.23	300	0.63
1020C-16H-5, 140-150	0.070	1.20	772.36	1075	1.39
1021D-1H-3, 140-150	0.085	1.58	8.99	80	8.90
1021C-5H-2, 140-150	0.074	1.30	162.90	180	1.10
1021C-9H-1, 140-150	0.082	1.23	309.98	320	1.03
1021C-18H-3, 140-150	0.067	0.77	694.24	900	1.30

Note: OCR = overconsolidation ratio.

REFERENCES

Holtz, R.D., and Kovacs, W.D., 1981. *An Introduction to Geotechnical Engineering:* Englewood Cliffs, NJ (Prentice-Hall).

Lyle, M., Koizumi, I., Richter, C., et al., 1997. *Proc. ODP, Init. Repts.,* 167: College Station, TX (Ocean Drilling Program).

MacKillop, A.K., Moran, K., Jarrett, K., Farrell, J., and Murray, D., 1995. Consolidation properties of equatorial Pacific Ocean sediments and their relationship to stress history and offsets in the Leg 138 composite depth sections. *In* Pisias, N.G., Mayer, L.A., Janecek, T.R., Palmer-Julson, A., and van Andel, T.H. (Eds.), *Proc. ODP, Sci. Results,* 138: College Station, TX (Ocean Drilling Program), 357–369.

Moran, K., 1997. Elastic property corrections applied to Leg 154 sediment, Ceara Rise. *In* Shackleton, N.J., Curry, W.B., Richter, C., and Bralower, T.J. (Eds.), *Proc. ODP, Sci. Results,* 154: College Station, TX (Ocean Drilling Program), 151–155.

Terzaghi, K., 1943. *Theoretical Soil Mechanics:* New York (Wiley).

Date of initial receipt: 20 April 1999
Date of acceptance: 5 August 1999
Ms 167SR-244

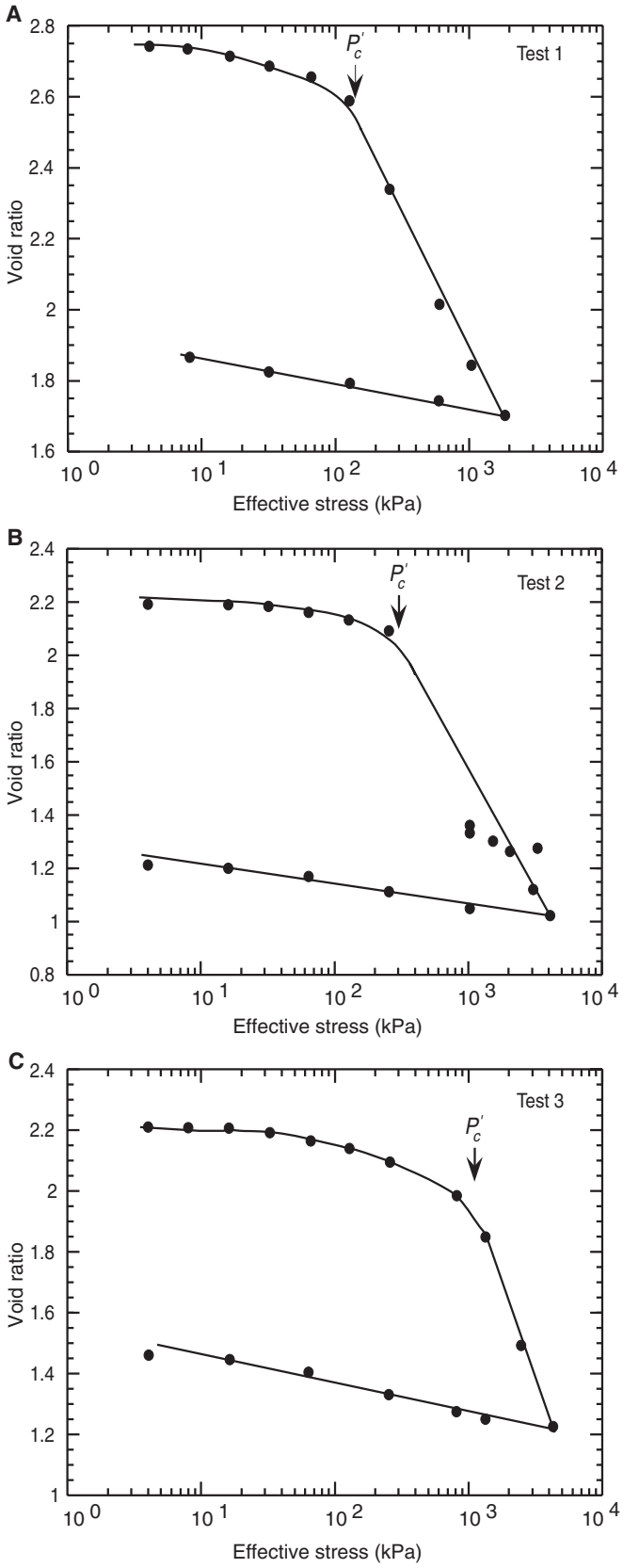

Figure 2. Consolidation plots for whole-round samples recovered from (**A**) Hole 1020D (5.95 mbsf), (**B**) Hole 1020C (92.75 mbsf), and (**C**) Hole 1020C (144.78 mbsf).

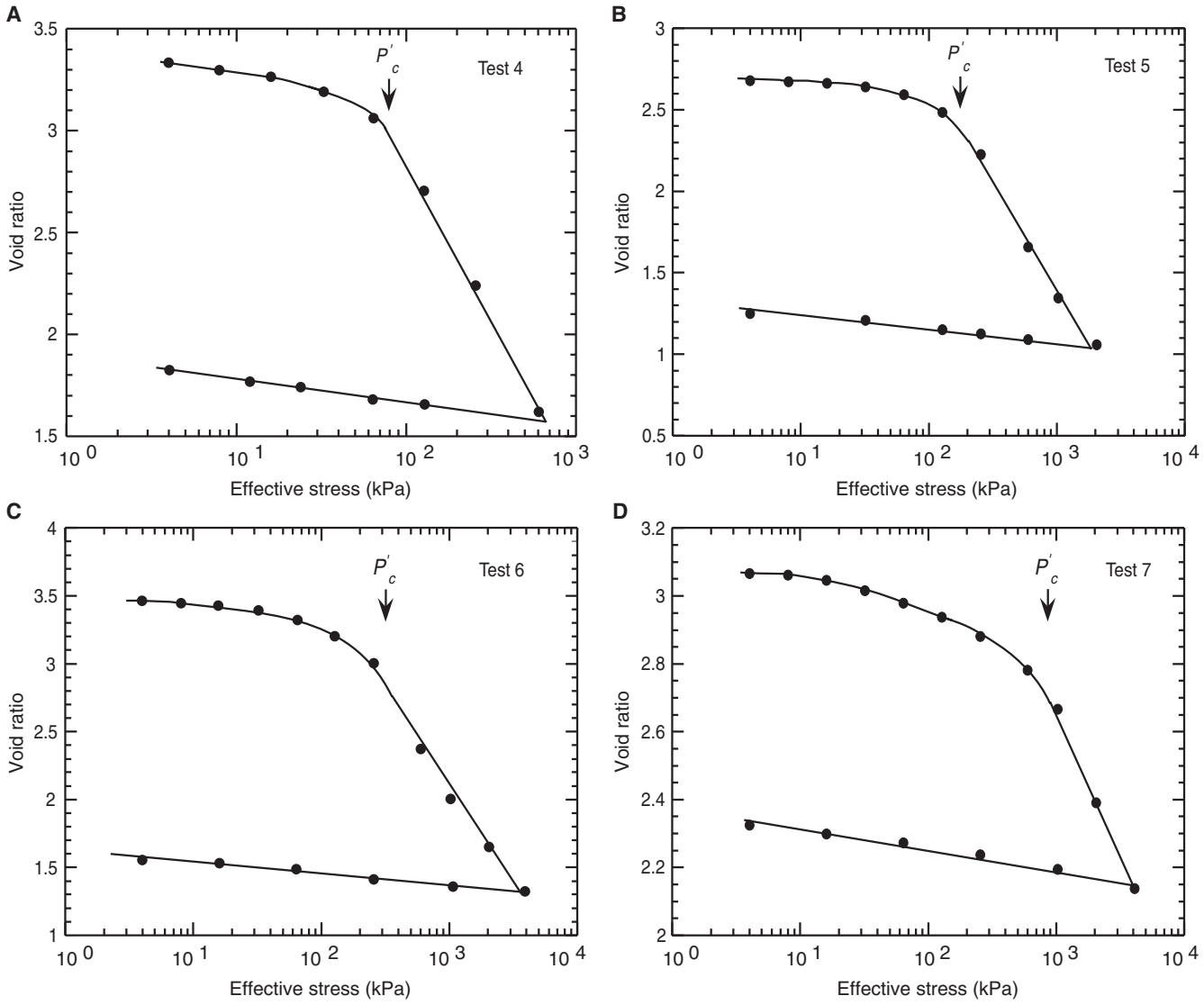

Figure 3. Consolidation plots for whole-round samples recovered from (**A**) Hole 1021D (54.45 mbsf), (**B**) Hole 1021C (34.05 mbsf), (**C**) Hole 1021C (70.55 mbsf), and (**D**) Hole 1020C (129.05 mbsf).

Table 3. Corrected index physical properties values for APC cores at Site 1020.

Core, section, interval (cm)	Midpoint depth (mbsf)	P'_0 (kPa)	Corrected void ratio	Corrected porosity (%)	Corrected density (g/cm^3)	Corrected dry density (g/cm^3)
167-1020B-						
1H-2, 30-32	2.55	10.14	3.099	75.603	1.470	0.679
1H-3, 30-32	4.05	16.63	2.549	71.821	1.509	0.755
1H-4, 30-32	5.55	23.47	2.565	71.948	1.534	0.778
1H-5, 30-32	7.45	31.65	2.694	72.931	1.506	0.742
2H-1, 80-82	9.10	39.77	2.242	69.152	1.573	0.845
2H-2, 30-32	10.35	45.27	2.576	72.035	1.517	0.761
2H-3, 30-32	11.85	51.52	2.644	72.558	1.491	0.731
2H-4, 30-32	13.35	58.57	2.341	70.070	1.549	0.812
2H-5, 30-32	14.85	64.76	2.612	72.315	1.487	0.729
2H-6, 30-32	16.75	73.95	2.156	68.310	1.564	0.845

This is a sample of the table that appears on the volume CD-ROM.

Table 4. Corrected index physical properties values for APC cores at Site 1021.

Core, section, interval (cm)	Midpoint depth (mbsf)	P'_0 (kPa)	Corrected void ratio	Corrected porosity (%)	Corrected density (g/cm^3)	Corrected dry density (g/cm^3)
167-1021B-						
1H-1, 30-32	0.60	2.34	2.947	74.666	1.462	0.681
1H-1, 90-92	1.35	5.33	3.052	75.323	1.473	0.685
1H-2, 30-32	2.55	8.97	4.310	81.166	1.366	0.523
1H-3, 30-32	4.05	13.78	4.087	80.344	1.385	0.550
1H-4, 30-32	5.55	19.47	3.358	77.051	1.451	0.646
1H-5, 30-32	7.05	24.86	3.418	77.365	1.429	0.622
1H-6, 30-32	8.05	28.60	3.197	76.175	1.444	0.648
2H-1, 30-32	9.05	32.62	3.142	75.859	1.476	0.683
2H-2, 30-32	10.55	38.02	3.401	77.276	1.429	0.623
2H-3, 30-32	12.05	44.85	2.549	71.825	1.534	0.780

This is a sample of the table that appears on the volume CD-ROM.

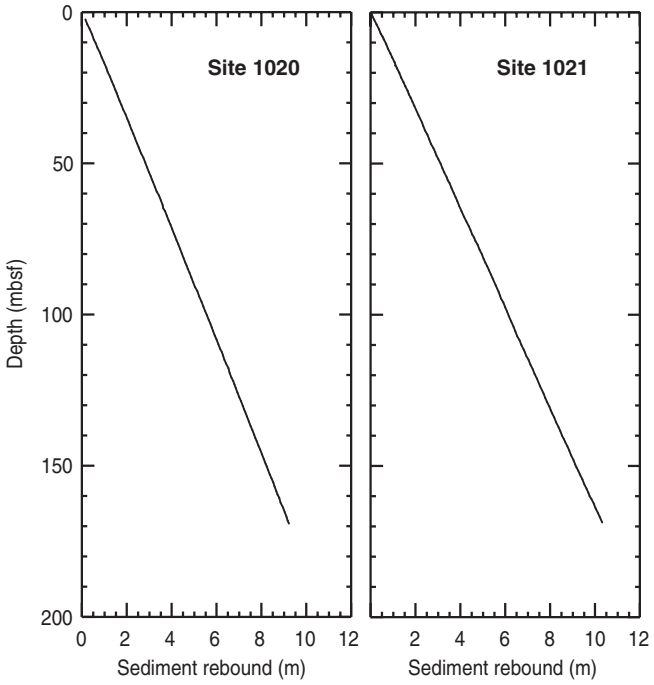

Figure 4. Length of sediment expansion plotted as a function of the shipboard depth scale (mbsf).

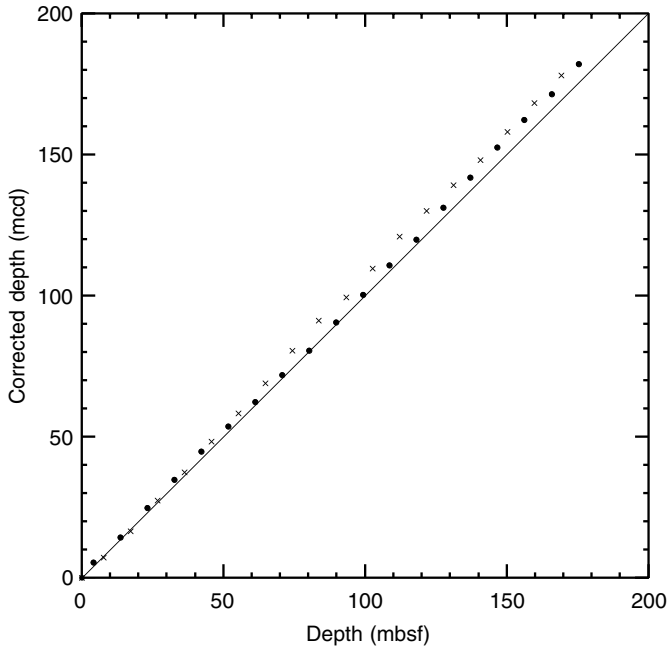

Figure 5. Comparison of the corrected mcd scale with the shipboard mbsf scale for Holes 1020B (crosses) and 1020C (solid circles).

Table 5. Meters composite depth (mcd) correction coefficients for Equation 8.

Site	Elastic rebound coefficient *a*	Elastic rebound coefficient *b*
1020	0.063	0.973
1021	0.066	0.986

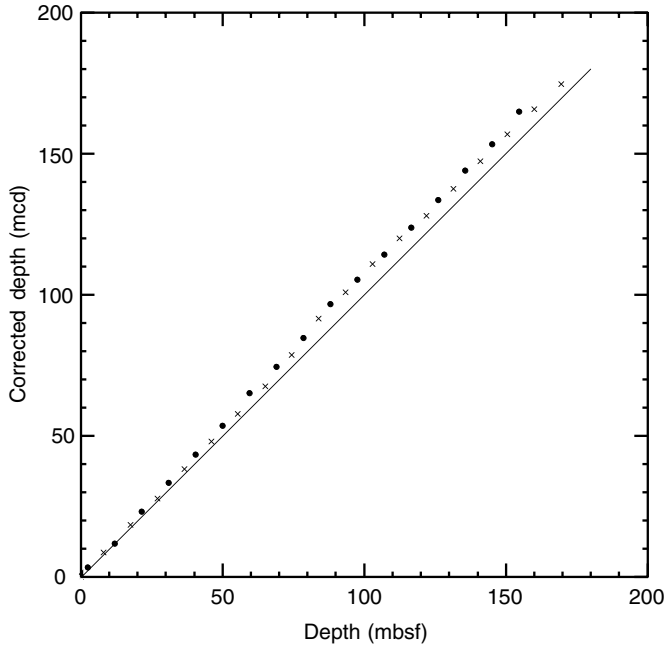

Figure 6. Comparison of the corrected mcd scale with the shipboard mbsf scale for Holes 1021B (crosses) and 1021C (solid circles).

Table 6. Contribution of sediment rebound to the depth offset between the mbsf and mcd scales at Site 1020.

Core, section	Depth (mbsf)	Mcd depth offset (m)	Sediment rebound (m)	Rebound contribution to the mcd offset (%)
167-1020B-				
1H-1	0.0	0.08	0.00	0.00
2H-1	7.8	–0.14	0.46	–330.87
3H-1	17.3	0.26	1.01	386.69
4H-1	26.8	2.08	1.54	73.99
5H-1	36.3	3.16	2.07	65.43
6H-1	45.8	4.92	2.59	52.68
7H-1	55.3	5.92	3.11	52.60
8H-1	64.8	7.71	3.63	47.12
9H-1	74.3	10.19	4.15	40.73
10H-1	83.8	12.05	4.67	38.72
11H-1	93.3	11.27	5.18	45.96
12H-1	102.8	12.44	5.69	45.75
13H-1	112.3	14.88	6.20	41.68
14H-1	121.8	14.98	6.71	44.81
15H-1	131.3	14.98	7.22	48.21
16H-1	140.8	14.93	7.73	51.77
17H-1	150.3	15.81	8.24	52.09
18H-1	159.8	17.13	8.74	51.03
167-1020C-				
1H-1	0.0	0.00	0.00	0.00
2H-1	4.3	1.30	0.26	19.96
3H-1	13.8	1.16	0.81	69.56
4H-1	23.3	2.72	1.34	49.38
5H-1	32.8	3.82	1.87	49.04
6H-1	42.3	4.82	2.40	49.78
7H-1	51.8	4.68	2.92	62.43
8H-1	61.3	4.29	3.44	80.23
9H-1	70.8	4.91	3.96	80.65
10H-1	80.3	4.55	4.48	98.37
11H-1	89.8	5.71	4.99	87.39
12H-1	99.3	6.35	5.50	86.66
13H-1	108.8	7.88	6.01	76.32
14H-1	118.3	7.88	6.52	82.80
15H-1	127.8	10.21	7.03	68.89
16H-1	137.3	11.92	7.54	63.27
17X-1	146.8	13.67	8.05	58.88
18X-1	156.3	14.37	8.56	59.54

Table 7. Contribution of sediment rebound to the depth offset between the mbsf and mcd scales at Site 1021.

Core, section	Depth (mbsf)	Mcd depth offset (m)	Sediment rebound (m)	Rebound contribution to the mcd offset (%)
167-1021B-				
1H-1	0.0	0.00	0.00	0.00
2H-1	8.0	1.18	0.51	43.17
3H-1	17.5	1.94	1.10	56.80
4H-1	27.0	2.50	1.69	67.59
5H-1	36.5	4.02	2.27	56.57
6H-1	46.0	4.76	2.86	60.02
7H-1	55.5	5.69	3.44	60.41
8H-1	65.0	6.55	4.02	61.32
9H-1	74.5	8.71	4.59	52.75
10H-1	84.0	12.75	5.17	40.56
11H-1	93.5	13.15	5.75	43.71
12H-1	103.0	14.31	6.32	44.19
13H-1	112.5	14.29	6.90	48.27
14H-1	122.0	13.43	7.47	55.63
15H-1	131.5	14.13	8.04	56.93
16H-1	141.0	14.95	8.62	57.64
17H-1	150.5	15.53	9.19	59.17
18H-1	160.0	15.41	9.76	63.34
167-1021C-				
1H-1	0.0	–0.08	0.00	0.00
2H-1	2.6	0.88	0.17	19.12
3H-1	12.1	0.44	0.77	174.09
4H-1	21.6	2.88	1.36	47.08
5H-1	31.1	4.12	1.94	47.14
6H-1	40.6	5.24	2.53	48.20
7H-1	50.1	6.64	3.11	46.80
8H-1	59.6	9.19	3.69	40.13
9H-1	69.1	9.64	4.27	44.26
10H-1	78.6	10.84	4.84	44.69
11H-1	88.1	13.96	5.42	38.83
12H-1	97.6	13.78	6.00	43.51
13H-1	107.1	13.75	6.57	47.79
14H-1	116.6	14.21	7.15	50.28
15H-1	126.1	15.09	7.72	51.15
16H-1	135.6	16.59	8.29	49.98
17H-1	145.1	16.99	8.86	52.17
18H-1	154.6	19.65	9.44	48.02